PN
PHYTONUTRIENTS

Information available at: infor@phytonutrients.pk
PHYTONutrients
Journal home page: https://phytonutrients.pk/index.php/pn

Lyceum Publisher

Anticancer Potential of *Diospyros kaki* (persimmon) polyphenols against AKT1 (6CCY): docking based *in silico* study

Ijaz Muhammad[1], Gul E Nayab[1], Noor Rahman[2], Sadaf Niaz[1], Abid Ali[1], Haroon Khan[3,*]

Citation: Ijaz Muhammad, Gul E Nayab, Noor Rahman, Sadaf Niaz, Abid Ali, Haroon Khan. Anticancer Potential of *Diospyros kaki* (persimmon) polyphenols against AKT1 (6CCY): docking based *in silico* study *PHYTONutrients* **2022**;01:57-68.
https://doi.org/10.62368/pn.v1i01.13

Editor: Michael Aschner

Received: 12th October
Accepted: 28th October
Published: November

[1] Department of Zoology, Abdul Wali Khan University Mardan, Mardan-23200, KP, Pakistan ijazmawkum@gmail.com ; nayabawkum@gmail.com ; sadaf@awkum.edu.pk; drabid@awkum.edu.pk
[2] Department of Biochemistry, Abdul Wali Khan University Mardan, Mardan-23200, KP, Pakistan. noorbiochemist@gmail.com
[3] Department of Pharmacy, Abdul Wali Khan University Mardan, Mardan-23200, Pakistan. haroonkhan@awkum.edu.pk

*Correspondence: haroonkhan@awkum.edu.pk

ABSTRACT: The elevation of AKT activity in many aggressive tumors, and AKT signaling is frequently compromised in various cancers. The range of AKT inhibitors' therapeutic effects extends beyond cancer management. AKT inhibitors may potentially be used to treat cancer. The study aims to find a potent drug compound from *D. kaki* polyphenols that could serve as an AKT1 inhibitor. *In silico* study using Molecular operating environment (MOE) software was employed to find the therapeutic potential of phytochemicals from *D. kaki* against AKT1 via molecular docking and drug-like properties. Results of the study revealed that acarbose (**compound 1**) has the highest docking score of -7.4615 with receptor protein 6CCY, followed by quercetin 3-O-glucoside (**compound 2**) with a docking score of -6.86404133 measured in terms of kcal/mol. Pocket residues involved in protein-ligand interaction was GLU234, GLU278, ASP292, ASN79, LYS276, LYS189, PHE161, HIS194, LYS179, ASP291, LYS158, GLU278. Thus, bioactive compounds from *D. kaki* may be a potentially novel anticancer agent by inhibiting AKT1.

Keywords: *Diospyros kaki*; AKT1; molecular docking; *in silico*; phytochemicals; anticancer.

1. Introduction

The AGC family of kinases includes AKT, protein kinase B (PKB), and a serine/threonine-specific protein kinase. Mammals have three AKT isoforms that are closely related to one another: AKT1, AKT2, and AKT3 (Santi *et al*., 2019; Hinz and Jücker, 2019). All of these AKT isoforms share a three-domain structure that includes an N-terminal pleckstrin homology (PH) domain that interacts with phosphatidylinositol-3-kinase

(PI3K), a C-terminal catalytic kinase domain that has an ATP-binding site, and a hydrophobic motif (HM) (Barile *et al*., 2010). The catalytic domain of AKT isoforms exhibits a high degree of sequence homology, but the other two domains exhibit some variation. AKT1 and AKT2 are present in all tissues, whereas AKT3 is mostly prevalent in the heart, kidney, and brain. AKT, a critical enzyme in the PI3K cascade, is essential for controlling various cellular processes. AKT has several important roles in the body, including promoting cell growth, cell cycle progression, cell survival, and inhibiting apoptosis by inactivating more than 20 pro-apoptotic proteins (Santi *et al*., 2019; Nitulescu *et al*., 2018; Altomare and Testa, 2005; Manning *et al*., 2002). AKT activity is elevated in many aggressive tumors, and AKT signaling is frequently compromised in various cancers. Consequently, these enzymes are viewed as prospective targets for creating new anticancer medications (Mundi *et al*., 2016; Dumble *et al*., 2014; Kumar *et al*., 2013). However, AKT inhibitors' therapeutic effects extend beyond cancer management. According to recent studies, AKT inhibitors may potentially treat neurological disorders, diabetes, obesity, cardiovascular conditions, idiopathic pulmonary fibrosis, and inflammatory and autoimmune diseases [Huang *et al*., 2018; Nitulescu *et al*., 2018; Hers *et al*., 2011]. At least seven AKT inhibitors are presented through various phases of clinical trials. (Song *et al*., 2019). Most of these drugs have undergone clinical testing, and because they bind to the catalytic region of the enzymes, they simultaneously block all three AKT isoforms (i.e., pan-AKT inhibitors). Allosteric inhibitors, however, were also created to increase selectivity towards one or more AKT isoforms (Narayan *et al*., 2017). As an illustration, an allosteric inhibitor with stronger selectivity for the AKT1 and AKT2 isoforms is BAY1125976. However, it has yet to be clinically proven that isoform-specific AKT inhibitors are superior to pan-AKT inhibitors (Song *et al*., 2019; Brown *et al*., 2017). However, it has already been established that when creating novel AKT inhibitors, bioactivity against all three isoforms should be taken into account.

Furthermore, because many natural products contain numerous bioactive chemicals, including alkaloids, polyphenols, and flavonoids, which have antioxidant and anti-mutagenic properties, they inhibit the proliferation of cancer cells (Zhou *et al*., 2014; Pan *et al*., 2010). Diospyros kaki, a persimmon, is a member of the Ebenaceae family of plants and is widely farmed in East Asia, including Korea, China, and Japan. Although D. kaki's fruits are frequently eaten as food due to their advantageous qualities, the plant's leaves are frequently utilized in traditional medicine (Choi *et al*., 2016). *D. kaki leaves are abundant in bioactive substances, such as polyphenols, flavonoids, and terpenoids* (Izuchi *et al*., 2009). Quercetin and kaempferol, as well as their glycoside, galactoside, or galloylated derivatives, are present in ethanol extracts of D. kaki leaves (Kim *et al*., 2015).

To date, it has been demonstrated that using machine learning-based (ML) technologies to design and find therapeutically effective medicines is a very effective strategy (Halder *et al*., 2019; Lo *et al*., 2018; 2016). Therefore, we need to research these new healthy natural ingredients and assess their effectiveness as cutting-edge cancer therapies. We evaluated the anticancer phytonutrients of *D. kaki's* via molecular docking studies to check the interactions of these compounds with AKT1 target.

2. METHODS AND MATERIALS

2.1. Target Retrieval and Ligand Preparation

The crystal structure of AKT1 protein (PDB ID:6CCY) with resolution 2.18Å (Parthasarathy et al. 2018) was retrieved from the Protein Data Bank (https://www.rcsb.org). The isolated compounds of *D. kaki L.* were used for a molecular docking study. The molecular structures of the reported compounds were drawn in ChemBioDraw Ultra 13.0, and all the structures were saved in mol files. The mol format of ligands was opened in Molecular Operating Environment (MOE) software (Chemical Computing Group Inc., 2016) (Version 2014.09) for 3D protonation and energy minimization and saved in MDB files for molecular docking. Roundabout 28 polyphenolic compounds have been reported in the literature for *D. kaki L.* (Direito 2021; Hossain 2021; Kwon 2021; Maulidiani 2018; Yaqub 2018; Butt 2015).

2.2. **Structure validation**

Ramachandran plot was generated to check and verify the protein's structure prior to docking. By evaluating parameters, including favored, allowed, and outlier regions of amino acid residues in the predicted protein structure, MOE software was used to construct Ramachandran plots for validating 6CCY protein structures. The Ramachandran plot was generated using MOE software using the PDB files of the protein from

the best model. For the projected model, a Ramachandran plot was produced.

2.2. Receptor Preparation

The MOE program was used to open the 6CCY PDB structure after it had been retrieved, and all of the water molecules were removed. 3D protein protonation and energy minimization were performed using the default MOE software parameters to obtain a stable protein structure.

2.3. Active Site Prediction

The active docking site was identified utilizing the MOE's site finder feature, which also served as a predictor of the active site. Utilizing the receptor's three-dimensional (3D) atomic coordinates, the Site Finder tool was used to determine potential active sites (6CCY protein). In order to choose dummy atoms from the receptor for probable docking sites for ligand binding, calculations must be made.

2.4. Molecular Docking

For docking purposes, the MDB ligand files were selected while keeping the MOE package default parameters such as placement: triangular matcher, rescoring 1: London dG, rescoring 2: GBVI/WSA, and refinement: Force field (Rahman et al. 2019). Ten conformations were created for each ligand, and the top-ranked conformations were selected based on docking score and residue interaction to evaluate lead compounds.

3. Results

The protein 6CCY consists of a total of 343 amino acid residues. The evaluation of crystal structure of the protein by Ramachandran plot showed most of the amino acid residues (97.37%) were found in the core region, eight (2.33%) were found in the allowed region, and only one amino acid, ASP324 (0.29%), was found in the outlier region, as shown in **Fig 1**.

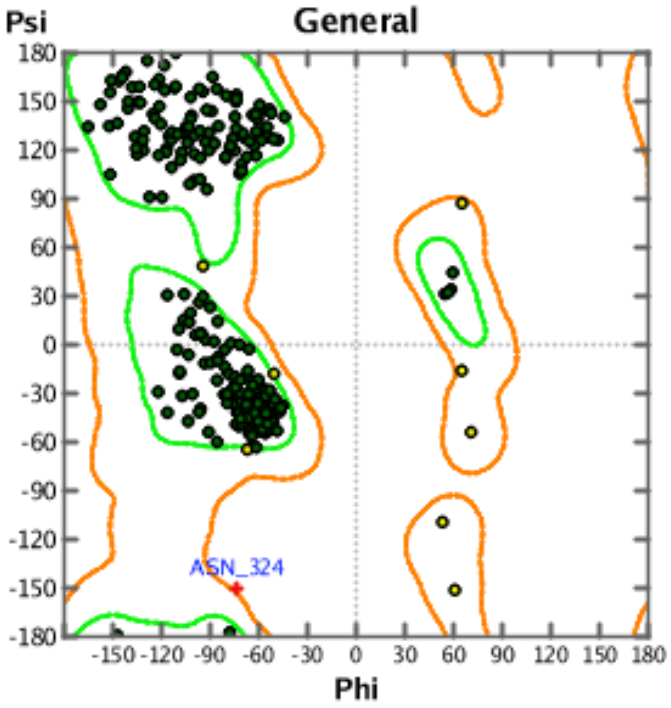

Figure 1. Structural analysis of the 6CCY protein by Ramachandran plot.

The active site (pocket) of 6CCY protein have LEU156, GLY157, LYS158, GLY159, PHE161, GLY162, LYS163, VAL164, ALA177, LYS179, ILE180, LEU181, ILE186, GLU191, HIS194, THR195, GLU198, LEU202, THR211, MET227, GLU228, GLU234, PHE236, PHE237, SER240, ARG241, ASP274, LYS276, LEU277, GLU278, ASN279, LEU280, MET281, THR291, ASP291, PHE291, GLY294, LEU295, THR312, GLU314, TYR315, GLU341, LEU347, TYR350, PHE438, ASP439, GLU441, PHE442.

Of the 28 docked compounds from *D. kaki L.*, 25 show interactions with the target protein. Three compounds did not show any interaction. Five compounds showed docking scores of more than 6 kcal/mol. The docking score of all docked compounds is shown in **Table 1**.

Table 1: Demonstrating the common name, chemical structure, docking score with target proteins, and ligand properties

	Name of compound	Compound structure	Docking score in kcal/mol	Ligand Properties
1	Acarbose	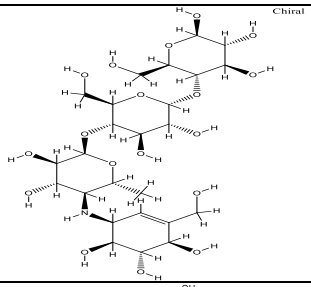	-7.4615	Toxic: no Rsynth: 72.73% Weight: 644.60 g/mol TPSA: 331.41 A^2 (don: 12, acc: 18) logP: -8.71 logS: 1.36
2	Quercetin 3-O-glucoside	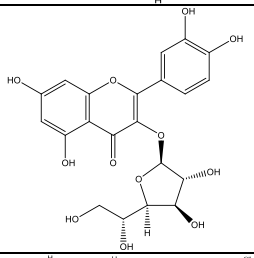	-6.86404133	Toxic: no Rsynth: 100% Weight: 464.38 g/mol TPSA: 206.60 A^2 (don: 8, acc: 11) logP: -8.71 logS: 1.36
3	Procyanidin	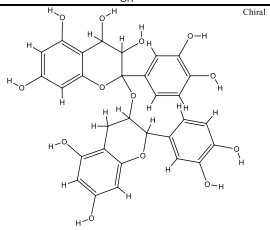	-6.55342913	Toxic: no Rsynth: 100% Weight: 594.52 g/mol TPSA: 229.99 A^2 (don: 10, acc: 13) logP: 3.24 logS: -4.02
4	Quercetin 3–2-galloylglucoside	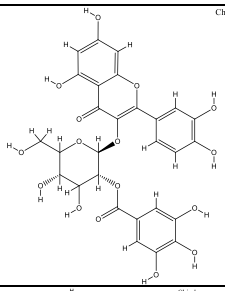	-6.20982599	Toxic: no Rsynth: 100% Weight: 615.48 g/mol TPSA: 276.19 A^2 (don: 9, acc: 14) logP: 3.24 logS: -4.02
5	kaempferol 3-(200-galloylglucoside	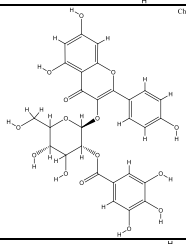	-6.17157125	Toxic: no Rsynth: 100% Weight: 599.48 g/mol TPSA: 255.96 A^2 (don: 8, acc: 13) logP: 0.98 logS: -4.28
6	Epigallocatechin gallate	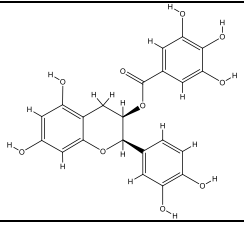	-5.95677948	Toxic: no Rsynth: 100% Weight: 458.37 g/mol TPSA: 197.37 A^2 (don: 8, acc: 10) logP: 2.33 logS: -2.67

7	Gallocatechin gallate	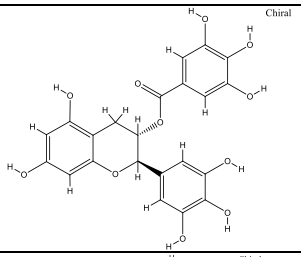	-5.83148289	Toxic: no Rsynth: 100% Weight: 458.37 g/mol TPSA: 197.37 A^2 (don: 8, acc: 10) logP: 2.33 logS: -2.67
8	Epicatechin gallate	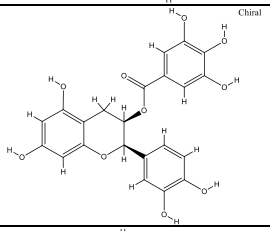	-5.82633543	Toxic: no Rsynth: 37.50% Weight: 442.38 g/mol TPSA: 177.14 A^2 (don: 7, acc: 9) logP: 2.62 logS: -3.03
9	Avicularin	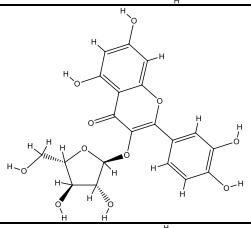	-5.7750802	Toxic: no Rsynth: 100% Weight: 434.35 g/mol TPSA: 186.37 A^2 (don: 7, acc: 10) logP: -0.09 logS: -2.75
10	Catechin gallate	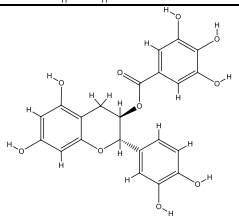	-5.61706924	Toxic: no Rsynth: 37.50% Weight: 442.38 g/mol TPSA: 177.14 A^2 (don: 7, acc: 9) logP: 2.62 logS: -3.03
11	Epi) catechin	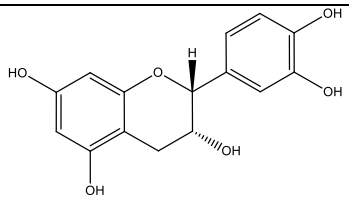	-5.51410484	Toxic: no Rsynth: 4.76% Weight: 290.27 g/mol TPSA: 110.38 A^2 (don: 5, acc: 6) logP: 1.64 logS: -1.74
12	Gallocatechin 3'-O-gallate	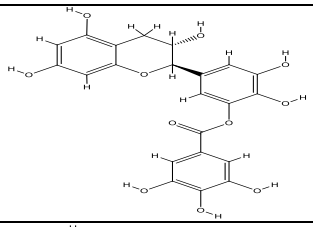	-5.51261759	Toxic: no Rsynth: 39.39% Weight: 458.37 g/mol TPSA: 197.37 A^2 (don: 5, acc: 6) logP: 1.98 logS: -2.76
13	Cyanidin	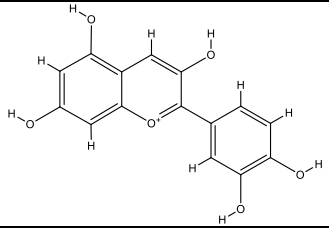	-5.43803072	Toxic: no Rsynth: 100% Weight: 287.25 g/mol TPSA: 114.29 A^2 (don: 5, acc: 5) logP: 2.91 logS: -3.69

14	Galangin	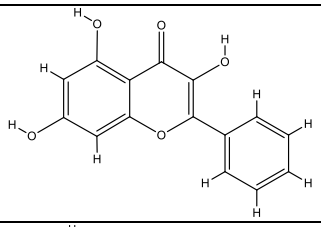	-5.35146093	Toxic: no Rsynth: 100% Weight: 270.24 g/mol TPSA: 86.99 A^2 (don: 3, acc: 4) logP: 2.60 logS: -3.50
15	Epi) gallocatechin	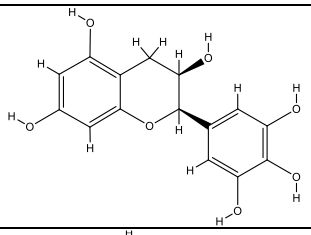	-5.29366398	Toxic: no Rsynth: 100% Weight: 306.27 g/mol TPSA: 130.61 A^2 (don: 6, acc: 7) logP: 1.35 logS: -1.37
16	Kaempferol-3-O-glucoside	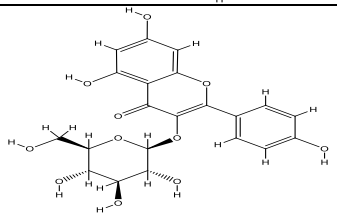	-5.33244085	Toxic: no Rsynth: 100% Weight: 447.37 g/mol TPSA: 189.20 A^2 (don: 6, acc: 10) logP: 0.00 logS: -2.98
17	Myricetin	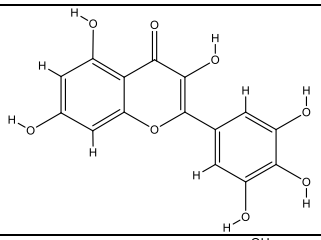	-5.09705639	Toxic: no Rsynth: 100% Weight: 318.25 g/mol TPSA: 147.68 A^2 (don: 6, acc: 7) logP: 1.72 logS: -2.41
18	Quercetin	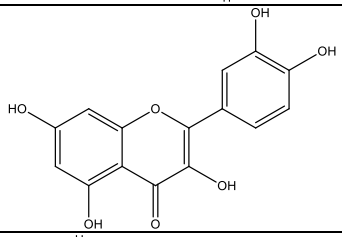	-5.03358841	Toxic: no Rsynth: 100% Weight: 302.24 g/mol TPSA: 127.45 A^2 (don: 5, acc: 6) logP: 2.01 logS: -2.77
19	Pelargonidin	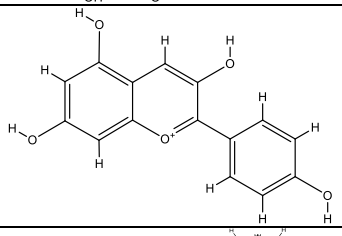	-4.76280403	Toxic: no Rsynth: 100% Weight: 271.25 g/mol TPSA: 94.04 A^2 (don: 4, acc: 4) logP: 3.20 logS: -4.05
20	Oleanolic acid	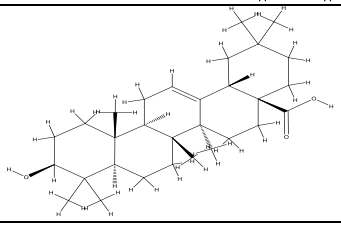	-4.63903522	Toxic: no Rsynth: 0.00% Weight: 455.70 g/mol TPSA: 60.36 A^2 (don: 1, acc: 3) logP: 5.90 logS: -8.88

21	Ellagic acid	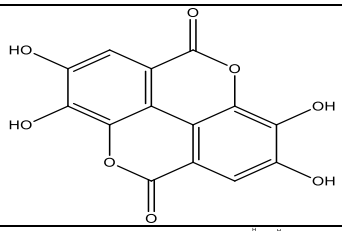	-4.60883141	Toxic: no Rsynth: 0.00% Weight: 302.19 g/mol TPSA: 133.52 A^2 (don: 4, acc: 6) logP: 1.24 logS: -4.12
22	Stigmasterol	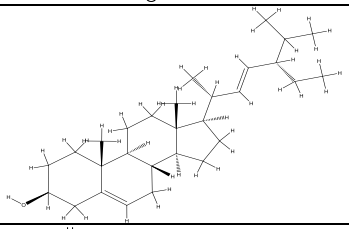	-4.56021881	Toxic: no Rsynth: 100% Weight: 412.70 g/mol TPSA: 20.23 A^2 (don: 1, acc: 3) logP: 7.80 logS: -10.83
23	Dihydroquercetin	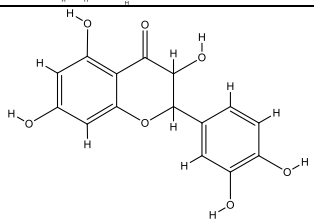	-4.48584414	Toxic: no Rsynth: 100% Weight: 304.25 g/mol TPSA: 127.45 A^2 (don: 5, acc: 7) logP: 1.28 logS: -2.01
24	Kaempferol	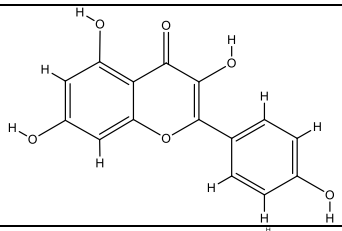	-4.40495872	Toxic: no Rsynth: 100% Weight: 286.24 g/mol TPSA: 107.22 A^2 (don: 4, acc: 5) logP: 2.31 logS: -3.14
25	Ursolic acid	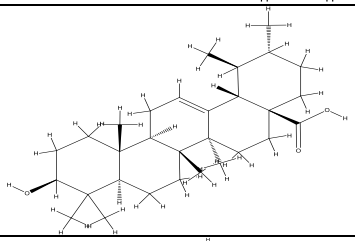	-4.1716671	Toxic: no Rsynth: 0.00% Weight: 455.70 g/mol TPSA: 60.36 A^2 (don: 1, acc: 3) logP: 5.90 logS: -8.88
26	Betulinic acid	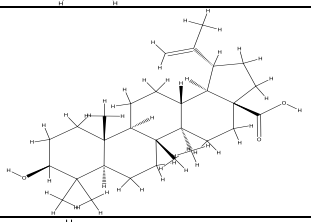	No docking	
27	Delphinidin	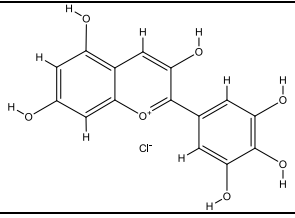	No docking	

28	Proanthocyanidin A2	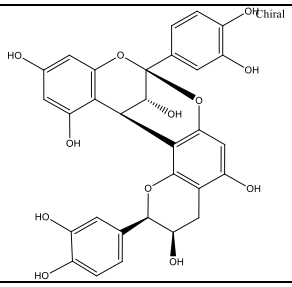	No docking	

Acarbose (**compound 1**) showed the highest docking score of -7.4615 kcal/mol with the target protein. GLU234, GLU278, and ASP292 residues of the target protein show three acidic (sidechain donor) interactions with OH moiety of the same benzene ring of **compound 1**. ASN79 also showed an acidic (side chain donor) interaction with the OH group of another benzene of docked ligand. LYS276 and LYS189 exhibit polar bonds (side chain acceptors) with the oxygen and OH moiety of the benzene ring of **compound 1**. The hydroxyl group of the benzene ring exhibits arene-H interactions with PHE161 and HIS194 of the target protein. LYS179 exhibits metal/ion contact with the oxygen moiety. All the 2D interactions are shown in **Figures 2a and 2b.**

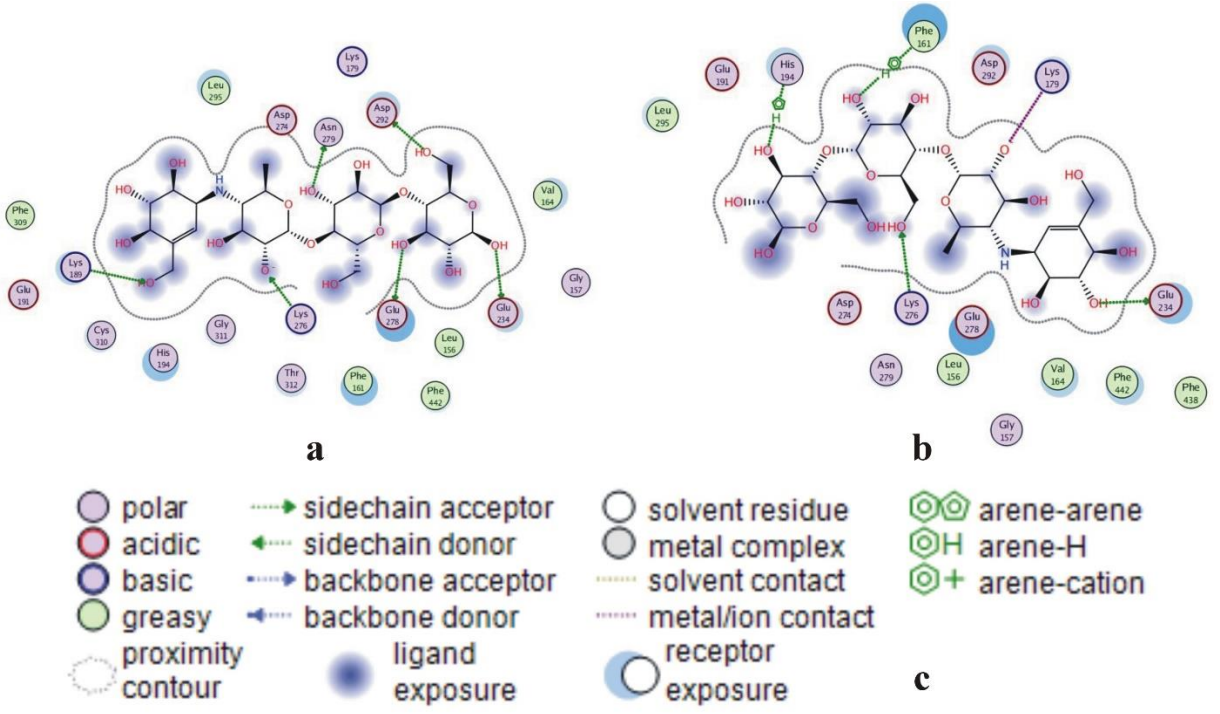

Figure 2. The a and b visualization of the 2D interaction of compound 1 with target protein 6CCY. The types of interactions are also shown in figure c.

Quercetin 3-O-glucoside (**compound 2**) shows a docking score of -6.86 kcal/mol with the target protein. The hydroxyl moiety of **compound 2** possesses two polar bonds (side chain acceptor) with GLU234 of the target protein. The hydroxy moiety has a polar contact (side chain acceptor) with ASP291. LYS158 and GLU278 also have good interactions with the ligand. All interactions are shown in **Figure 3**.

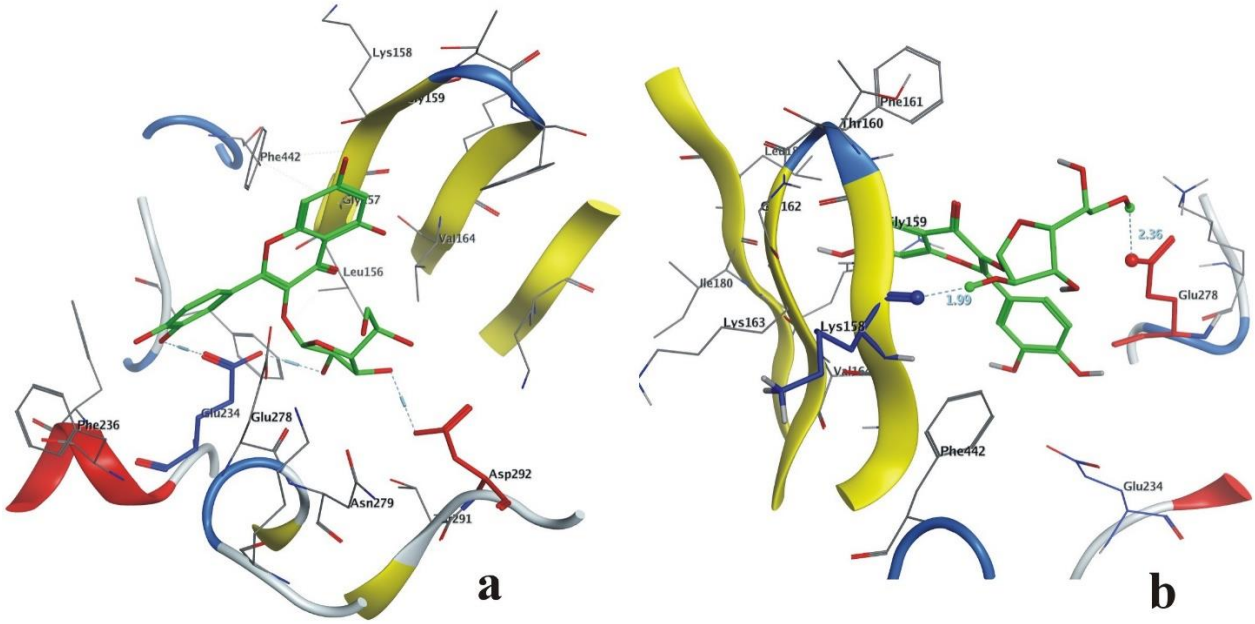

Figure 3. The a and b schematic 3D structures of the potent compounds acarbose 6CCY receptor and bond distance in Å. The receptor's inhibitory binding sites display chemical interactions with the ligand atoms and associated amino acids.

4. Discussion

Alternatives that may be examined include substances made from natural sources. Particularly, edible natural products have bioactive ingredients with fewer adverse effects (Vuorela *et al*., 2004; Firn *et al.,* 2003; Bindseil *et al.,* 2001). Molecular docking was employed to perform the library's virtual screening of phytochemicals from *D. kaki L.* against the targeted protein (6CCY). The current study is the first report of *D. kaki L.* polyphenols tested against 6CCY proteins. The current study results **show that compound 1** (acarbose) has the highest binding energy (-7.4615) with the target protein. According to Adinortey *et al*., acarbose is the most popular T2DM therapy option. Acarbose, a medication approved by the FDA, binds to the target protein with a binding energy of 34.3 kJ/mol. Twelve hydrogen bond interactions between acarbose and the protein's seven residues, Asp282, Asn524, Phe525, Arg600, Asp616, and His764, were also discovered. Except for His764, which had a 3.05 Å hydrogen bond length, all of its hydrogen bond lengths were below 3.0Å (Adinortey *et al*., 2022). The **compound 1** binding energy is much lower than that previously reported by Adinortey *et al*. Han *et al*. demonstrated that administration of acarbose caused Akt levels to rise substantially. It has been shown that diabetic rats given acarbose displayed enhanced insulin-induced Akt activation in adipocytes (Han *et al*., 2017). The present *in silico* study reported that **compound 1** showed good binding energy with AKT1 protein and can act as a potent inhibitor of the protein. A study by Xu *et al*. reported that the amino acids GLU277, HIS351, and ASP352, which are a part of the catalytic residues of isomaltase and were thought to play important roles in the catalytic mechanism as the corresponding residues of GLU275, HIS348, and ASP349 in -glucosidase, were found surrounding acarbose, a competitive inhibitor against α-glucosidase (Xu *et al*., 2019). **Compound 1** shows interaction with different amino acid residues from the study of Xu *et al*., as the binding pocket of both target proteins possesses different amino acids. A study by Zhang *et* al. documented that the glide score for acarbose in the active N-terminal maltase-glucoamylase (2QMJ) was −7.34 kcal/mol. For C-terminal maltase-glucoamylase (3TOP), the glide score for acarbose in the active site (site 3) was −8.00 kcal/mol. For N-terminal sucrase-isomaltase (3LPP), the glide score for acarbose in the active site (site 3) was −7.13 kcal/mol (Zhang *et* al., 2017). The glide score reported by Zhang *et*

al. for the different target proteins is almost identical to the docking score reported in the current study. The interaction of acarbose and amylase involves six conventional H-bonds with five amino acids (Gln63, Asn105, Thr163, His299, and Asp300). Similarly, acarbose and glucosidase interactions showed four H-bonds with Tyr301, Gln302, Asn306, and Met331 (Sarma *et al*., 2021). The results of Lee et al. *in vitro* study hypothesized that quercetin-3-O glucoside would prevent the local spread of pancreatic tumors caused by various growth stimuli (Lee et al., 2018). In the current *in silico* study, it is proved that compound 2 could act as a potential inhibitor of AKT1 in cervical cancer. Balogun *et al*. reported that with a binding energy of -6.635 kcal/mol, quercetin-3-O-glucoside has the highest affinity for the active site of BRCA-1. Active site research revealed the following essential amino acids to be involved in the protein-ligand interaction: ASN 1678, ASN 1774, GLY 1656, LEU 1657, GLN 1779, LYS 1802, SER 1655, PHE 1662, ARG 1699, GLU 1698, and VAL 1654 (Balogun *et al*., 2021). The results of the current study align with the reports of Balogun *et al*. in terms of docking scores. However, the binding residues reported in both studies are different because of the protein structure. Both target proteins possess different pockets.

5. Conclusion

As a result of the rising instances of adverse effects brought on by synthetic pharmaceuticals, there is an increased demand worldwide for natural products, which has created a need for the scientific verification of conventional medical practices. A well-known healthy food called *D. kaki* has some bioactive chemicals, which have pharmacological effects. In Among the phytochemicals of the *D, kaki,* acrabose and quercetin 3-O-glucoside have strong binding affinity with AKT1 target. By inhibiting AKT1, bioactive chemicals from *D. kaki* may be a potentially novel anticancer drug. More research is necessary to comprehend the mechanisms underlying this advantageous effect brought on by the administration of phytochemicals.

Conflict of Interest

The authors declare no conflict of interest.

Author's contribution: All authors equally contributed.

Acknowledgment: Nil

Funding: No external funding

References

Adinortey, C.A., Kwarko, G.B., Koranteng, R., Boison, D., Obuaba, I., Wilson, M.D. and Kwofie, S.K., 2022. Molecular Structure-Based Screening of the Constituents of Calotropis procera Identifies Potential Inhibitors of Diabetes Mellitus Target Alpha Glucosidase. Current Issues in Molecular Biology, 44(2), pp.963-987.

Altomare, D.A. and Testa, J.R., 2005. Perturbations of the AKT signaling pathway in human cancer. Oncogene, 24(50), pp.7455-7464.

Balogun, T.A., Buliaminu, K.D., Chukwudozie, O.S., Tiamiyu, Z.A. and Idowu, T.J., 2021. Anticancer potential of Moringa oleifera on BRCA-1 gene: Systems biology. Bioinformatics and Biology Insights, 15, p.11779322211010703.

Barile, E., De, S.K., Carlson, C.B., Chen, V., Knutzen, C., Riel-Mehan, M., Yang, L., Dahl, R., Chiang, G. and Pellecchia, M., 2010. Design, Synthesis, and Structure-Activity Relationships of 3-Ethynyl-1 H-indazoles as Inhibitors of the Phosphatidylinositol 3-Kinase Signaling Pathway. Journal of medicinal chemistry, 53(23), pp.8368-8375.

Bindseil, K.U., Jakupovic, J., Wolf, D., Lavayre, J., Leboul, J. and van der Pyl, D., 2001. Pure compound libraries; a new perspective for natural product-based drug discovery. Drug Discovery Today, 6(16), pp.840-847.

Brown, J.S. and Banerji, U., 2017. Maximising the potential of AKT inhibitors as anticancer treatments. Pharmacology & therapeutics, 172, pp.101-115.

Butt, M.S., Sultan, M.T., Aziz, M., Naz, A., Ahmed, W., Kumar, N. and Imran, M., 2015. Persimmon (Diospyros kaki) fruit: hidden phytochemicals and health claims. EXCLI journal, 14, p.542.

Choi, M.S., Jeong, M.J., Park, Y.B., Kim, S.R. and Jung, U.J., 2016. The leaf of Diospyros kaki Thumb ameliorates renal oxidative damage in mice with type 2 diabetes. Preventive Nutrition and Food Science, 21(4), p.378.

Direito, R., Rocha, J., Sepodes, B. and Eduardo-Figueira, M., 2021. From Diospyros kaki L. (Persimmon) phytochemical profile and health impact to new product perspectives

and waste valorization. Nutrients, 13(9), p.3283. M. González, C., Hernando, I. and Moraga, G., 2021. In Vitro and In Vivo Digestion of Persimmon and Derived Products: A Review. Foods, 10(12), p.3083.

Dumble, M., Crouthamel, M.C., Zhang, S.Y., Schaber, M., Levy, D., Robell, K., Liu, Q., Figueroa, D.J., Minthorn, E.A., Seefeld, M.A. and Rouse, M.B., 2014. Discovery of novel AKT inhibitors with enhanced anti-tumor effects in combination with the MEK inhibitor. PloS one, 9(6), p.e100880.

Firn, R.D. and Jones, C.G., 2003. Natural products–a simple model to explain chemical diversity. Natural product reports, 20(4), pp.382-391.

Halder, A.K. and Cordeiro, M.N.D.S., 2019. Development of multi-target chemometric models for the inhibition of class I PI3K enzyme isoforms: A case study using QSAR-Co tool. International journal of molecular sciences, 20(17), p.4191.

Han, X., Deng, Y., Yu, J., Sun, Y., Ren, G., Cai, J., Zhu, J. and Jiang, G., 2017. Acarbose accelerates wound healing via Akt/eNOS signaling in db/db mice. Oxidative medicine and cellular longevity, 2017.

Hers, I., Vincent, E.E. and Tavaré, J.M., 2011. Akt signalling in health and disease. Cellular Signalling, 23(10), pp.1515-1527.

Hinz, N. and Jücker, M., 2019. Distinct functions of AKT isoforms in breast cancer: a comprehensive review. Cell Communication and Signaling, 17(1), pp.1-29.

Hossain, U., Das, A.K., Ghosh, S. and Sil, P.C., 2020. An overview on the role of bioactive α-glucosidase inhibitors in ameliorating diabetic complications. Food and chemical toxicology, 145, p.111738.

Huang, X., Liu, G., Guo, J. and Su, Z., 2018. The PI3K/AKT pathway in obesity and type 2 diabetes. International Journal of Biological Sciences, 14(11), p.1483.

Izuchi, R., Takahashi, H. and Inada, Y., 2009. Preparing a carotenoid polyphenol-enriched extract from the peel of persimmon, Diospyros kaki Lf. Bioscience, Biotechnology, and Biochemistry, 73(12), pp.2793-2795.

Kim, K.A., Kang, S.W., Ahn, H.R., Song, Y., Yang, S.J. and Jung, S.H., 2015. Leaves of persimmon (Diospyros kaki Thunb.) ameliorate N-methyl-N-nitrosourea (MNU)-induced retinal degeneration in mice. Journal of agricultural and food chemistry, 63(35), pp.7750-7759.

Kumar, A., Rajendran, V., Sethumadhavan, R. and Purohit, R., 2013. AKT kinase pathway: a leading target in cancer research. The Scientific World Journal, 2013.

Kwon, J., Park, J.E., Lee, J.S., Lee, J.H., Hwang, H., Jung, S.H., Kwon, H.C. and Jang, D.S., 2021. Chemical Constituents of the Leaves of Diospyros kaki (Persimmon). Plants, 10(10), p.2032.

Lee, J., Lee, J., Kim, S.J. and Kim, J.H., 2016. Quercetin-3-O-glucoside suppresses pancreatic cancer cell migration induced by tumor-deteriorated growth factors in vitro. Oncology reports, 35(4), pp.2473-2479.

Lima, A.N., Philot, E.A., Trossini, G.H.G., Scott, L.P.B., Maltarollo, V.G. and Honorio, K.M., 2016. Use of machine learning approaches for novel drug discovery. Expert opinion on drug discovery, 11(3), pp.225-239.

Lo, Y.C., Rensi, S.E., Torng, W. and Altman, R.B., 2018. Machine learning in chemoinformatics and drug discovery. Drug discovery today, 23(8), pp.1538-1546.

Manning, G., Whyte, D.B., Martinez, R., Hunter, T. and Sudarsanam, S., 2002. The protein kinase complements of the human genome. Science, 298(5600), pp.1912-1934.

Maulidiani, M., Mediani, A., Abas, F., Park, Y.S., Park, Y.K., Kim, Y.M. and Gorinstein, S., 2018. 1H NMR and antioxidant profiles of polar and non-polar extracts of persimmon (Diospyros kaki L.)–metabolomics study based on cultivars and origins. Talanta, 184, pp.277-286.

Mundi, P.S., Sachdev, J., McCourt, C. and Kalinsky, K., 2016. AKT in cancer: new molecular insights and advances in drug development. British Journal of Clinical Pharmacology, 82(4), pp.943-956.

Narayan, R.S., Fedrigo, C.A., Brands, E., Dik, R., Stalpers, L.J., Baumert, B.G., Slotman, B.J., Westerman, B.A., Peters, G.J. and Sminia, P., 2017. The allosteric AKT inhibitor MK2206 shows a synergistic interaction with chemotherapy and radiotherapy in glioblastoma spheroid cultures. BMC Cancer, 17(1), pp.1-8.

Nitulescu, G.M., Van De Venter, M., Nitulescu, G., Ungurianu, A., Juzenas, P., Peng, Q., Olaru, O.T., Grădinaru, D., Tsatsakis, A., Tsoukalas, D. and Spandidos, D.A., 2018. The Akt pathway in oncology therapy and

beyond. International journal of oncology, 53(6), pp.2319-2331.

Pan, L., Chai, H. and Kinghorn, AD, 2010. The continuing search for antitumor agents from higher plants. Phytochemistry Letters, 3(1), pp.1-8.

Parthasarathy, S., Henry, K., Pei, H., Clayton, J., Rempala, M., Johns, D., De Frutos, O., Garcia, P., Mateos, C., Pleite, S. and Wang, Y., 2018. Discovery of chiral dihydropyridopyrimidinones as potent, selective and orally bioavailable inhibitors of AKT. Bioorganic & medicinal chemistry letters, 28(10), pp.1887-1891.

Rahman, N.; Muhammad, I.; Gul-E-Nayab; Khan, H.; Aschner, M.; Filosa, R.; Daglia, M. Molecular Docking of Isolated Alkaloids for Possible α-Glucosidase Inhibition. Biomolecules 2019, 9, 544.

Santi, S.A., Douglas, A.C. and Lee, H., 2010. The Akt isoforms, their unique functions and potential as anticancer therapeutic targets.

Sarma, P.P., Gurumayum, N., Verma, A.K. and Devi, R., 2021. A pharmacological perspective of banana: Implications relating to therapeutic benefits and molecular docking. Food & Function, 12(11), pp.4749-4767.

Song, M., Bode, A.M., Dong, Z. and Lee, M.H., 2019. AKT as a Therapeutic Target for CancerChallenging Cancer Therapy by Targeting AKT. Cancer Research, 79(6), pp.1019-1031.

Vuorela, P., Leinonen, M., Saikku, P., Tammela, P., Rauha, J.P., Wennberg, T. and Vuorela, H., 2004. Natural products in the process of finding new drug candidates. Current medicinal chemistry, 11(11), pp.1375-1389.

Xu, L., Li, W., Chen, Z., Guo, Q., Wang, C., Santhanam, R.K. and Chen, H., 2019. Inhibitory effect of epigallocatechin-3-O-gallate on α-glucosidase and its hypoglycemic effect via targeting PI3K/AKT signaling pathway in L6 skeletal muscle cells. International journal of biological macromolecules, 125, pp.605-611.

Yaqub, S., Farooq, U., Shafi, A., Akram, K., Murtaza, M.A., Kausar, T. and Siddique, F., 2016. Chemistry and functionality of bioactive compounds present in persimmon. Journal of Chemistry, 2016.

Zhang, B.W., Li, X., Sun, W.L., Xing, Y., Xiu, Z.L., Zhuang, C.L. and Dong, Y.S., 2017. Dietary flavonoids and acarbose synergistically inhibit α-glucosidase and lower postprandial blood glucose. Journal of agricultural and food chemistry, 65(38), pp.8319-8330.

Zhou, Y., Zhang, A.H., Sun, H., Yan, G.L. and Wang, X.J., 2014. Plant-derived natural products as leads to antitumor drugs. Plant Science Today, 1(2), pp.46-61.